buildings

MDPI

Article

Seismic Response of a Structure Equipped with an External Viscous Damping System

Antonio Sabino *, Antonio Mannella and Andrea Matteo de Leo

Italian National Research Council, Construction Technologies Institute, 67100 L'Aquila, Italy; mannella@itc.cnr.it (A.M.); ing.andrea.deleo@gmail.com (A.M.d.L.)

* Correspondence: sabino@itc.cnr.it

Received: 29 November 2019; Accepted: 14 January 2020; Published: 22 January 2020

Abstract: The aim of this research is to evaluate the effectiveness of a seismic retrofit technique that involves the introduction of energy dissipation devices properly connected to an existing structure through a system of cables and levers, which are employed to amplify total or inter-story drift at device end. One of the main topics related to the introduction of energy dissipation devices, lies in the choice of their optimal setting within the structure to maximize the effectiveness without producing functionality limitations. The achievement of these objectives is, therefore, linked, regardless of the type adopted, to the amount of energy dissipated in each cycle, directly proportional to the displacement magnitude to which the device is subject. Many configurations proposed in the literature and currently adopted in professional practice provide additional dissipation systems variously connected to braces installed inside the structural frame and, therefore, able to exploit the inter-story drift produced by seismic input. The proposed system exploits top displacements of the structure with respect to the foundation level, transferred to the device through a system of cables properly configured and amplified with leverage. This paper represents the first step of the research, in which simple single degree of freedom (SDOF) or two degrees of freedom (2-DOF) models are taken into account to evaluate the effects of the introduction of the proposed system in terms of reducing the seismic demand on the structure, proceeding to a parametric analysis to obtain initial indications for the design of the system in relation to the geometric and inertial characteristics of the original structure.

Keywords: seismic retrofit; viscous damping; earthquake; existing structures

1. Introduction

The introduction of seismic energy dissipation devices within existing structures represents an important seismic protection system widely adopted for framed structures. The deformability of these structures generally allows them, in fact, to exploit inter-story drifts to activate the devices and achieve consistent levels of dissipation of input energy. Many configurations and geometrical arrangements [1–3] have been proposed in order to optimize the devices' location, generally applied in series to a bracing placed inside the frame mesh and able to transfer to the device a fraction of the inter-story drift, depending on their geometric configuration. Therefore, it is clear that the deformability of the structure is an essential requirement for the effectiveness of dissipation systems. For situations where structures are not sufficiently flexible, interesting solutions have been developed by several authors, including a cable system solution (damped cable system, DCS), initially proposed by the research team of the University of Buffalo [4,5], and further developed [6–9] also as part of a research project funded by the European Commission, named SPIDER (strand prestressing for internal damping of earthquake response). The system consists of a pre-stressed high-grade steel cable, composed of greased and sheathed unbonded strands in standard production, whose lower end is connected to

a fluid-viscous damper fixed to the foundation of the building. The cable has sliding connections at the level of the decks, where it undergoes deviations until it connects with the roof. This cable arrangement allows the total displacement measured at the top of the structure to be transmitted to the dissipation the device, increasing the building's dissipative capacity and reducing the number of devices required. At the same time, the deviation of the cable in correspondence of each deck allows a reaction that balances seismic lateral loads to be transferred to it. Likewise, dissipation systems designed to increase displacements at the dissipation system end have been proposed by various authors [10–12] and generally consist of levers or pulley systems able to amplify inter-story displacement. The system proposed in this paper uses a system of steel cables capable to transmit a portion of the total roof displacement of the building to the foundation where, by means of a system of displacement amplification, a resulting amplified displacement is transferred to the damper. Considering a simple shear frame, the proposed system is configured according to the following scheme in Figure 1. The cable used (6) is fixed with clamps (7) at the upper ends of the floor; the cable, therefore, is arranged in an X configuration along the diagonals of the frame and diverted at the base of the columns by pulleys (4). The cable then runs horizontally along the base of the frame; in this area it is connected to the end of a lever arm (1), to the opposite end of which the dissipation device is connected (2). The particular configuration of the cable, which runs along both diagonals of the building's elevation, continuing without interruption at foundation level, also allows the same to be always active in both directions of seismic loads. The portion of the cable placed on the diagonal in tension (blue wire), in fact, exerts a recall action on the cable portion placed along the compressed diagonal (red wire), not allowing deflection. The configuration described above, is suitable for use on existing structures, without the need for demolition of the infills and expensive restoration of finishes or systems.

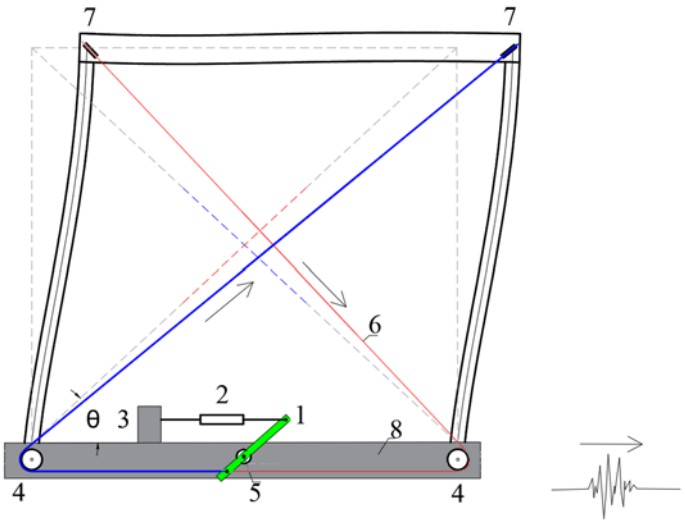

Figure 1. Conceptual model of simple 1-floor frame structure equipped with proposed system: 1 lever arm; 2 viscous damper (VD); 3 contrast; 4 pulleys; 5 pin; 6 wire; 7 clamp; 8 foundation.

The use of a displacement amplification system like that described, therefore, allows the usual limitations in the use of additional dissipation systems usually inserted inside the structural frames to be overcome, as it is effective even for limited displacements, thanks to the introduction of leverage, displacements are transmitted amplified to the device, increasing the amount of dissipated energy.

2. Mechanical Model

For the evaluation of the behavior of a structure equipped with the proposed cable dissipation system, a simple two degrees of freedom (DOF) system is considered, represented in the following

Figure 2, which can be representative of a single-story frame in which whole mass is concentrated in the beam. The bare structure has its own internal damping, assumed to be $\xi = 0.05$, and inertial characteristics, such as mass m_2 and natural frequency ω_2, from which the value of the dissipation coefficient c_2 is then obtained. The model thus described is equipped with an additional damping system, with a linear viscous dissipation device, described by the following general equation:

$$Fd = c_1 \dot{u_d} = \alpha_d c_2 \dot{u_d} \tag{1}$$

with $\dot{u_d}$ velocity at the device end and Fd device damping force.

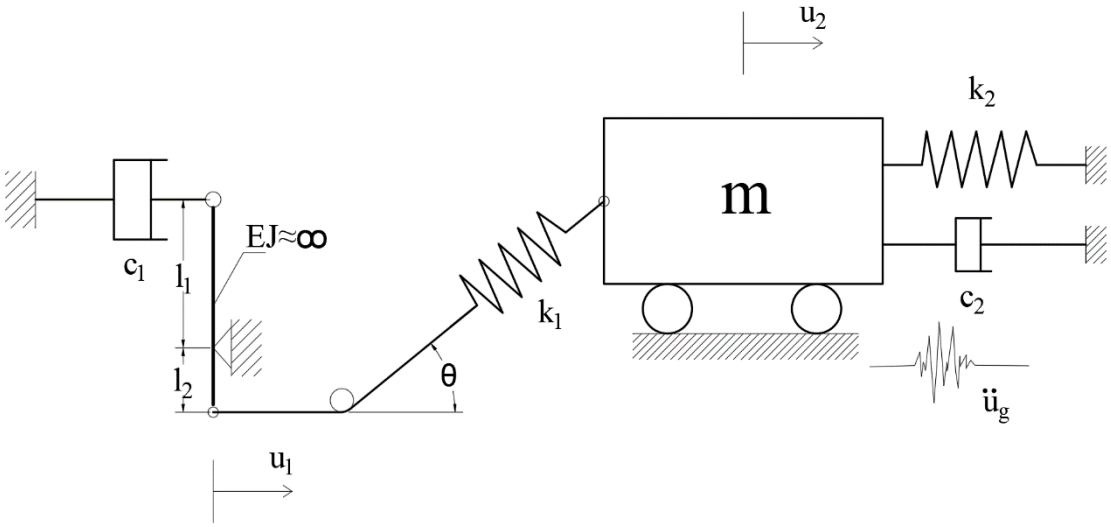

Figure 2. Mechanical model of a two degrees of freedom (2-DOF) structure equipped with the proposed system.

The damping coefficient is then expressed as a function of the internal damping of the structure through the parameter α_d. With reference to the stiffness characteristics of the system, the structure stiffness k_2 and the stiffness of the elements constituting the additional dissipation system, i.e., the cable and the leverages, k_1, are defined; actually, as shown below, the main stiffness component is represented by the cable extensional stiffness. As said, from the examination of the Figure 1 results that, in both directions of displacement, the part of the cable connecting the clamp placed in the direction of displacement with the lever arm is in tension (blue wire), while the remaining ones are not stressed (red wire) if friction in pulleys is neglected. In the evaluation of the extensional stiffness, therefore, it is necessary to refer to a length of the cable equal to half of the whole length. At this research stage the component related to the real viscous device elastic stiffness has been neglected, considering it is rigid and neglecting friction in pulleys, pin etc. Added stiffness k_1 has, therefore, been expressed as a function of the stiffness of the bare structure through the coefficient α_k:

$$k_1 = \alpha_k k_2 \tag{2}$$

Finally, the amplification ratio produced by the leverage is defined through:

$$\alpha_M = \frac{l_1}{l_2} \tag{3}$$

The equations of motion have been obtained by following the Lagrangian approach. The total kinetic energy of the system is given by:

$$T = \frac{1}{2} m \left(u_2(t) + X_g(t) \right)^2 \tag{4}$$

where $x_g(t)$ is the time law of the base input. The total potential energy of the system is given by:

$$U = \frac{1}{2}k_2u_2(t)^2 + \frac{1}{2}k_1(u_2(t)\cos(t) - u_1(t))^2 \quad (5)$$

The Lagrangian is then:

$$L = T - U \quad (6)$$

The equation of motion are finally obtained as:

$$\frac{d}{dt}\left(\frac{\partial L}{\partial q_i}\right) - \frac{\partial L}{\partial q_i} = Q_{k,i}\ (i, 1, 2) \quad (7)$$

where q_i are the generalized coordinates (i.e., u_1 and u_2) while $Q_{k,i}$ are the generalized non-conservative forces.

The equation of motion finally reads:

$$m\ddot{u}_2(t) + k_2u_2(t) + \cos\theta k_1(u_2(t)\cos\theta - u_1(t)) + c_2u_2(t) = -m\,\ddot{x}_g(t) \quad (8)$$

In Equation (8) the term $\cos\theta$ appears necessary to consider the real configuration of the cable, placed diagonally. The angle θ represents the inclination of the frame diagonal, depending on the length ratios between the columns and the beam. As it can easily guess, the smaller the angle with respect to the horizontal, formed by the diagonal, the greater will be the component of the total horizontal displacement of the structure transferred to the cable. The above is a simplification, which is acceptable in the case of small displacements with respect to the structural dimensions and involving infinitesimal variations of the angle θ during the motion of the system.

In order to consider the effect of the deformability of the components of the system (cable, leverage, etc.), in addition to the displacement of the structure u_2, a further degree of freedom, u_1, was introduced, which represents the displacement of the viscous device, through which it can differentiate the displacement to which the leverage is subject, from such transferred by structure to the cable. In the case of cable and leverage, both with infinite stiffness, extensional for the first one and flexural for the second one, the two displacements would be identical. The introduction of the u_2 displacement, moreover, allows to evaluate the effect of the cable stiffness on the system performances.

Therefore, Equation (8) contains the two unknown displacements, u_1 and u_2, for the determination of which it is necessary to introduce the following relation, that describes precisely the effect of the deformability of the cable placed in series to the dissipation device and that goes to constitute the second equation of the motion of the system:

$$\alpha_M c_1u_1(t) - k_1(u_2(t)\cos\theta - u_1(t)) = 0 \quad (9)$$

Replacing Equations (1),(2),(8) and (9) we obtain the equations of the motion as a function of the parameters α_M, α_d, α_k :

$$\begin{cases} m\ddot{u}_2(t) + k_2u_2(t) + \cos\theta\alpha_k k_2(u_2(t)\cos\theta - u_1(t)) + c_2u_2(t) = -m\,\ddot{x}_g(t) \\ \alpha_M\alpha_d c_2u_1(t) - \alpha_k k_2(u_2(t)\cos\theta - u_1(t)) = 0 \end{cases} \quad (10)$$

Proceeding as follows:

$$\omega_2^2 = \frac{k_2}{m_2} \quad (11)$$

$$\xi = \frac{c_2}{2\,m_2\omega_2} \quad (12)$$

The system Equation (10) turns into:

$$\begin{cases} \ddot{u}_2(t) + \omega_2^2 u_2(t) + \cos\theta\alpha_k\omega_2^2(u_2(t)\cos\theta - u_1(t)) + 2\xi\omega_2 u_2(t) = -\ddot{x}_g(t) \\ 2\alpha_M\alpha_d \cdot \xi \cdot \omega_2 \cdot u_1(t) - \alpha_k\omega_2^2(u_2(t)\cos\theta - u_1(t)) = 0 \end{cases} \quad (13)$$

Through the system of differential Equation (13), the dynamics of the system are completely defined. In particular:

$$\omega_2 = \sqrt{\frac{k_2}{m_2}} \quad (14)$$

$$\omega_{2d} = \sqrt{\frac{k_2(\alpha_k\cos\theta + 1)}{m_2}} \quad (15)$$

$$\zeta = \frac{c_2(1 + \alpha_d\alpha_M)}{2m_2\omega_{2d}} \quad (16)$$

$$\omega_{2diss} = \omega_{2d}\sqrt{1 - \zeta^2} \quad (17)$$

The natural frequency of the bare structure is represented by Equation (14); Equation (15) represents the frequency of the structure equipped with the system without damping; Equation (16) is the value assumed by the damping ratio considering both the structure internal damping, c_2 and the additional damping produced by the dissipation device, c_1. Finally, Equation (17) provides the value of the frequency of the damped system. The ratio between the natural frequencies of the bare system and the damped system leads to the following relationship:

$$\frac{\omega_{2diss}}{\omega_2} = \sqrt{(\alpha_k\cos\theta + 1)\left(1 - \zeta^2\right)} \quad (18)$$

from which it can be deduced that the introduction of the system leads on the one hand to an increase in the natural frequency of the structure proportional to the coefficients α_k and on the other hand to a reduction due to the effect of dissipation by means of Equation (9). The result of the two described effects will define the resulting dynamic response of the structure. Generally, for the range of possible values for the α_k, α_d and α_M coefficients the resulting effect produces a stiffening of the structure (for example for a structure with $\omega_2 = 20$ and values of $\alpha_k = 0.5$, $\alpha_d = 2$, $\alpha_M = 5$, increases in the natural frequency of the system of 15% are obtained).

Assuming an harmonic base input in the form:

$$\ddot{x}_g(t) = P\sin\Omega t \quad (19)$$

where P is the amplitude or maximum value of the force and Ω its forcing frequency

The DE (differential equation) system Equation (13) turn into:

$$\begin{cases} \ddot{u}_2(t) + \omega_2^2 u_2(t) + \cos\theta\alpha_k\omega_2^2(u_2(t)\cos\theta - u_1(t)) + 2\xi\omega_2 u_2(t) = -P\sin\Omega t \\ 2\alpha_M\alpha_d\xi\omega_2 u_1(t) - \alpha_k\omega_2^2(u_2(t)\cos\theta - u_1(t)) = 0 \end{cases} \quad (20)$$

and can be solved in closed form or numerically. In this case was performed a numerical integration, via Newmark-beta method [13], setting $\beta = 2$ and $\gamma = 3/2$ (backward finite differences method). For the purposes of the following analyses, a simple 2-DOF structure is taken in account, as reference, consisting of a 2D shear frame with 10,000 kg total mass and 8000 kN/m flexural stiffness of the columns. Columns have a 4 m height (H), while the beam is 5 m long (B), the configuration is such that the diagonal cable forms an angle with respect to the horizontal (in not deformed configuration) equal to:

$$\theta = \cot\frac{B}{H} = 0.675 \; = \; 38.69^\circ \quad (21)$$

Considering the great importance on the motion of the system, of the frequency content of the forcer with respect to the natural frequency of the system, it seems appropriate to consider most severe conditions, i.e., the resonance ones:

$$\Omega = \omega_{2diss} \tag{22}$$

These conditions, in fact, maximize effects in terms of acceleration and displacement on the structure. The following Figure 3 shows the results of an analysis conducted on the bare structure (BS—bare structure) and on the same structure equipped with the dissipation system described (DS–damped structure), adopting for the parameters α_M, α_k, α_d, respectively, the values 10, 1, 2 ($\omega_{2dss} = 23.3$rad). As it is clearly visible, considerable reductions are obtained both in the relative acceleration with respect to the base and in the relative displacement. The reduction of actions in terms of acceleration and displacement can be quantified by parameters γ_d and γ_a, defined gain factors, which quantify efficiency of the system and defined as follows:

$$\gamma_d = \frac{u_{BS}(t)_{max} - u_{DS}(t)_{max}}{u_{BS}(t)_{max}} \gamma_a = \frac{a_{BS}(t)_{max} - a_{DS}(t)_{max}}{a_{BS}(t)_{max}} \tag{23}$$

with $u_{BS}(t)_{max}$, maximum value of bare structure displacement and $u_{DS}(t)_{max}$ maximum value of damped system displacement and $a_{BS}(t)_{max}$, $a_{DS}(t)_{max}$ maximum value of damped system displacement, respectively, for the bare system and damped system. In the configuration shown, γ_d and γ_a assume values of 0.575 and 0.376, respectively.

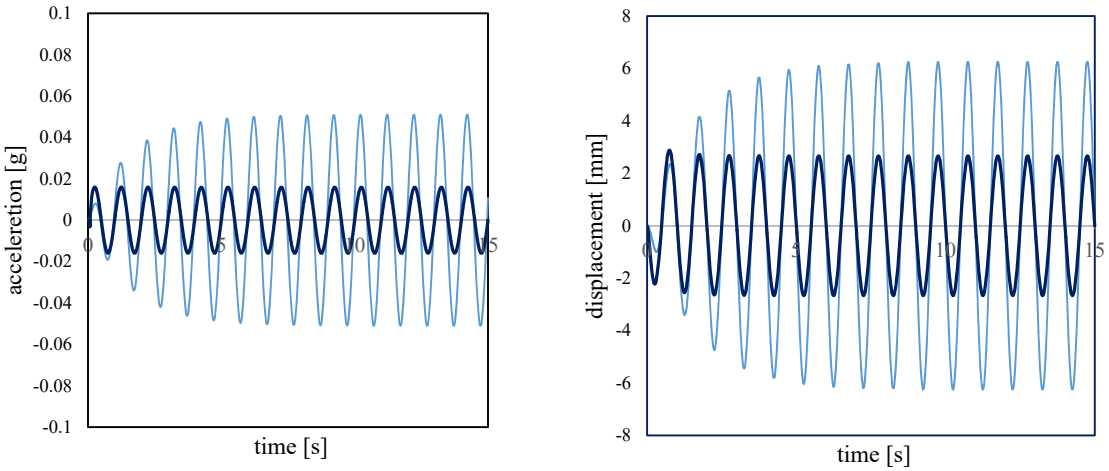

Figure 3. Relative acceleration (**a**) and displacement (**b**) respectively of bare single degree of freedom (SDOF) structure (BS—light blue line) and viscous damped SDOF Structure (DS—deep blue line) subjected to sinusoidal force.

In the case of a Multiple degree of freedom (MDOF) system, the equations system, in matricial form, turn into:

$$\mathbf{M}\ddot{u} + \mathbf{C}u + \mathbf{K}u = -\mathbf{M}\iota\ddot{u}_g \tag{24}$$

with $\ddot{u}_g$ ground acceleration and ι influence vector.

Stiffness and damping matrix assume the following forms:

$$K = \begin{bmatrix} (k_2 + k_1 \cdot \cos\theta_1(\alpha_{k1} \cdot \cos\theta_1 + 1)) & -k_2 & -(k_1 \cdot \alpha_{k1}) & 0 & 0 & 0 & 0 & 0 & \cdots & \cdots & 0 \\ -k_2 & (k_3 + k_2 \cdot \cos\theta_2(\alpha_{k2} \cdot \cos\theta_2 + 1)) & -k_3 & -(k_2 \cdot \alpha_{k2}) & 0 & 0 & 0 & 0 & \cdots & \cdots & 0 \\ 0 & -k_3 & (k_3 + k_2 \cdot \cos\theta_2(\alpha_{k2} \cdot \cos\theta_2 + 1)) & -k_4 & -(k_3 \cdot \alpha_{k3}) & 0 & 0 & 0 & \cdots & \cdots & 0 \\ & \cdots & \cdots & \cdots & \cdots & \cdots & \cdots & \cdots & \cdots & \cdots & 0 \\ & 0 & 0 & 0 & -k_i & (k_{i+1} + k_i \cdot \cos\theta_i(\alpha_{ki} \cdot \cos\theta_i + 1)) & -k_{i+1} & -(k_i \cdot \alpha_{ki}) & 0 & \cdots & 0 \\ & \cdots & \cdots & \cdots & \cdots & \cdots & \cdots & \cdots & \cdots & \cdots & 0 \\ & 0 & 0 & 0 & 0 & \cdots & \cdots & \cdots & -k_n & (k_n \cdot \cos\theta_n(\alpha_{kn} \cdot \cos\theta_n + 1)) & 0 \\ & 0 & 0 & 0 & 0 & \cdots & \cdots & \cdots & 0 & \alpha_{kn} \cdot k_n & \end{bmatrix} \tag{25}$$

$$C = \begin{bmatrix} c_1 + c_2 & -c_2 & 0 & \cdots & 0 & 0 & 0 & 0 \\ -c_2 & c_2 + c_3 & -c_3 & \cdots & 0 & 0 & 0 & 0 \\ 0 & 0 & c_1 \cdot \alpha_{d1} \cdot \alpha_{M1} & \cdots & 0 & 0 & 0 & 0 \\ \cdots & \cdots & \cdots & \cdots & \cdots & \cdots & \cdots & \cdots \\ 0 & 0 & 0 & \cdots & -c_i & c_i + c_{i+1} & -c_{i+1} & 0 \\ \cdots & \cdots & \cdots & \cdots & \cdots & \cdots & \cdots & \\ 0 & 0 & 0 & \cdots & 0 & 0 & c_n \cdot \alpha_{dn} \cdot \alpha_{Mn} & \end{bmatrix} \quad (26)$$

with symbols meaning reported in the following Figure 4.

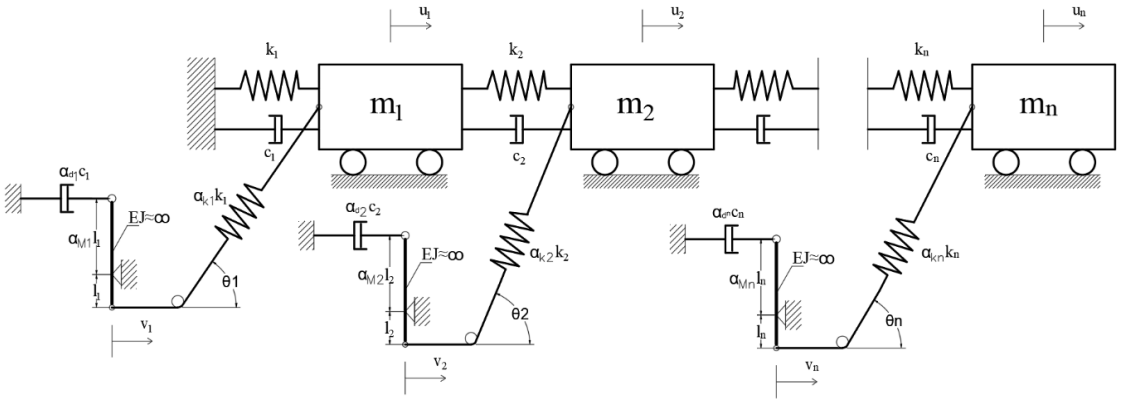

Figure 4. Mechanical model of a MDOF structure equipped with the proposed system.

The mechanical model reported in Figure 4 is related to a real n-story shear-type structure, with cables linking each story with foundation level (see Figure 5 for the case of a 2-story structure).

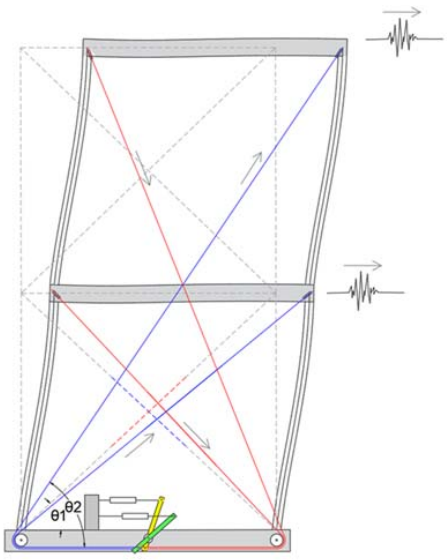

Figure 5. Conceptual model of a 2-story frame structure equipped with proposed system.

3. Results

3.1. Parametric Analysis

The previous introduction of parameters α_k and α_d allows a parametric analysis to be carried out in order to investigate the behaviour of the system when the damper properties (in terms of damping coefficient) and the stiffness of the cable (in relation to the stiffness of the bare structure) vary. In the case of infinite stiffness of the cable ($k \simeq \infty \rightarrow \alpha_k \simeq \infty$), the displacement of the damper terminal would

be exclusively a function of the amplification ratio produced by the leverage (α_M) and of the angle formed by the cable placed diagonally to the frame, with the horizontal. From (20) we can see that with angles close to 0° ($\cos\theta \simeq 1$), the horizontal displacement of the frame is transferred completely to the cable and then amplified to the damper. This configuration is difficult to achieve, with the cable close to the structure and without connections to external rigid elements, because it would require a very large structure if compared to their height. In the same way, the configurations that provide for angles close to 90° ($\cos\theta \simeq 0$) significantly reduce the rate of displacement transferred to the cable, which instead tends to rotate around the base pulley. The most recurrent configurations are those that see comparable dimensions of the columns height and of the beam length and, therefore, angles $\theta \simeq 45°$ and efficiency in the transfer of the horizontal displacement close to 70%. On the other hand, considering the opposite condition, namely infinitely flexible cable ($k \simeq 0 \rightarrow \alpha_k \simeq 0$) from (20) we see that most of the displacement of the structure does not reach the viscous damper because of high cable deformations, so high to completely absorb the displacement of the structure. This situation is similar to the one of the bare structure, without the dissipation system.

Intermediate values of cable stiffness ($0.1 < \alpha_k < 1$), involve the development of the cable elongation that can be considered as a "loss" influencing the efficiency of the system and moreover the dynamics of the structure equipped with it, through Equation (15).

The variation of the damping coefficient of the viscous damper, expressed as a function of the internal damping of the structure, produces even more consistent effects as its value increases, because of the fact that maintaining the hypothesis of the linear viscous damper, the force opposed by the device is a linear function, exclusively, of the difference in speed between its two terminals.

As noted in Equation (17), the value assumed by the damping coefficient of the viscous damper also has effects on the dynamic behavior of the structure, since it tends to make it more flexible as the value of the damping coefficient increases. The adoption of viscous devices with very low damping coefficient, while allowing high displacements, produces modest values of the energy dissipated for each cycle, although the adoption of leverage is able to amplify by α_M the value of the component of input energy dissipated by the system.

Finally, the value of α_M directly affects the dissipation properties of the system; as already noted, in fact, as the amplification ratio of the leverage increases, the displacements of the viscous damper are amplified (net of losses due to the cable deformability and the geometric configuration of the system, through the angle θ) as well as the velocity of the device terminal connected to the cable. It is important to underline that, in this phase, for the sake of simplicity, the contributions related to leverage and the dissipation device deformability and friction present between leverage connection and the pulleys have been neglected. Another phenomenon to be considered is the contribution to the cable deformability of thermal expansion or constant stress deformation. The presence, indeed, of an inflected cable is able to produce the loss of a large part of the displacement of the structure, which will be used to stretch the same before being transferred to the viscous device terminal. This deficiency, however, is largely controllable, providing the cable with a given pre-tension and combining the viscous damper device with a fuse element able to block movements up to a threshold tension in the cable and to not produce displacements in the damper. Alternatively, an active tensioning system could be adopted, capable of verifying, at fixed intervals of time, the tensioning state in the cable and provide for any tensioning, when necessary. For this reason, the present study maintains the simplifying hypothesis of a cable not subject to deflection.

In the light of the above considerations, the results of a parametric analysis are illustrated, in which, with reference to the benchmark structure described above, the dissipation system under study is introduced, by varying the parameters α_M, α_k and α_d within a range of plausible values in relation to the dimensional limits of the cable and dissipation devices currently available on the market, with the structure subject to a sinusoidal force, with frequency Ω equal to the resonance frequency of the structure ω_{2diss} and monitoring the variation of accelerations and maximum displacements in terms of gain factors, γ_d and γ_a, defined in Equation (23).

From the examination of the gain maps reported in Figure 6, it can be seen that as the stiffness of the cable increases, the efficiency of the damping system increases (due to the reduction of the extensional deformation partly absorbing structure displacements) for system with high α_M values. For a low α_M values system, the gain factors are not sensitive to the increase in cable stiffness, except for very low α_k values. The increase in the damping coefficient of the dissipation device produces, for low α_M values, a general increase in the efficiency of the system (with a reduction in displacements). Increasing the α_M values (>10), the gain factor γ_d is progressively less sensitive to α_d increase.

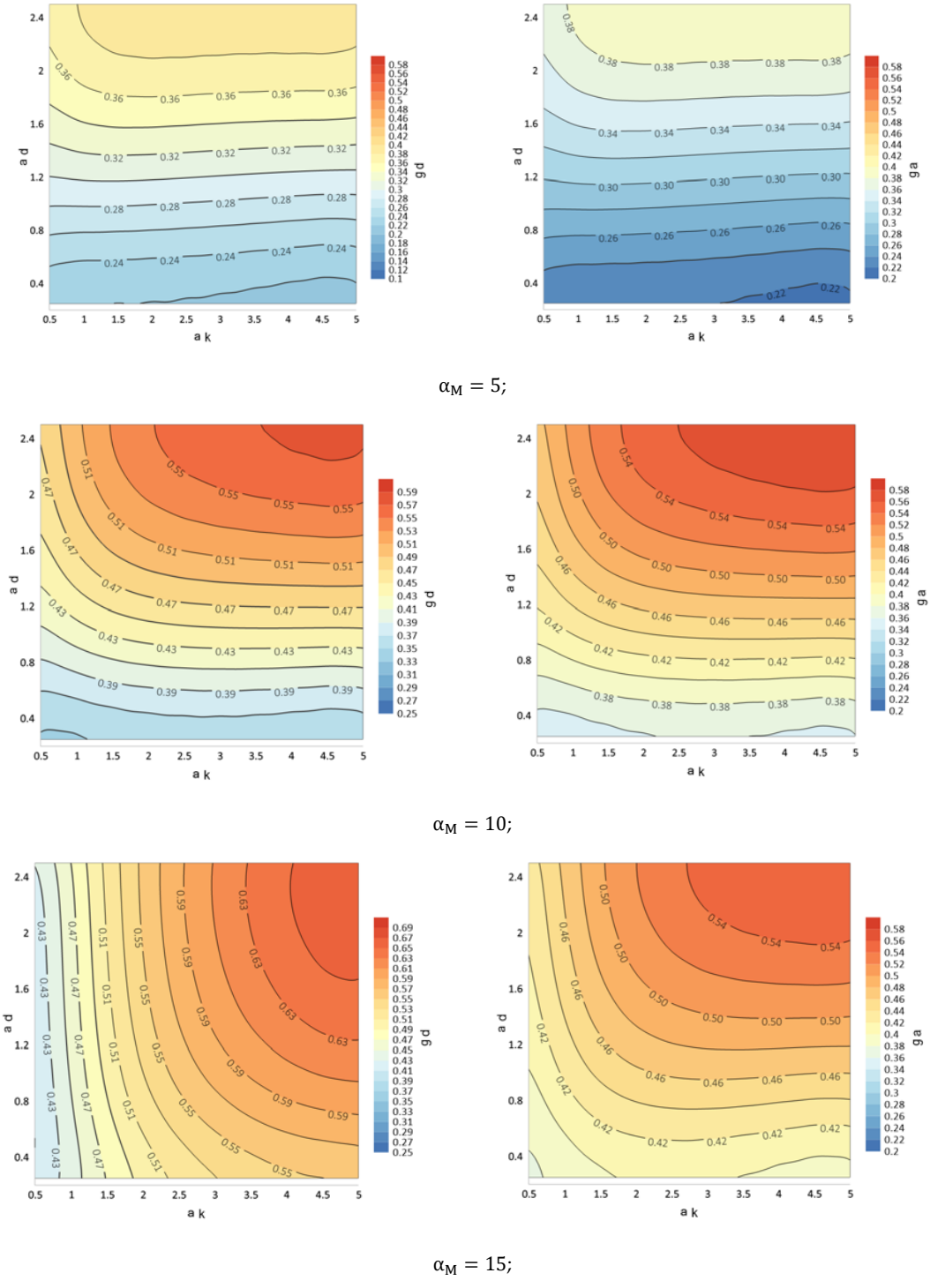

Figure 6. Gain maps in terms of γ_d (**left**) and γ_a (**right**) for various α_M values.

This circumstance derives from the composition of two opposite tendencies to which the structure is subject: as the damping constant of the dissipation system increases, the force exerted by the device increases, according to the provisions of the constitutive law exemplified in Equation (1), but at the same time the displacements u_1 at device end are reduced; on the contrary, as the force exerted by the device decreases by α_d reduction, the displacements u_1 increases (Figure 7). The optimal point is determined by the combination of F_d and displacement able to maximize the energy dissipated in each cycle.

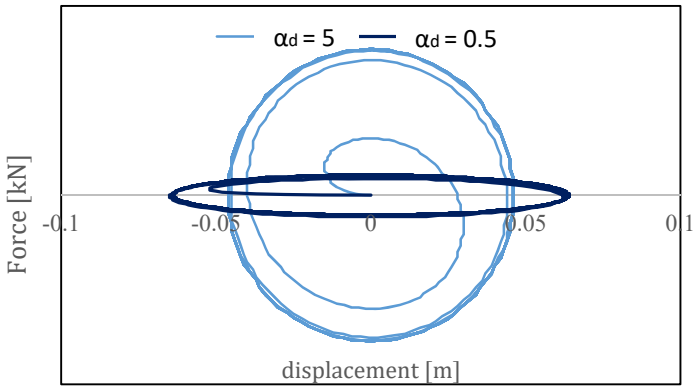

Figure 7. Viscous dissipative loops for sinusoidal force in viscous damper with $\alpha_d = 0.5$ and $\alpha_d = 5$.

The same principle is followed by the value assumed by the gain factors when varying α_M; the increase of the amplification coefficient (α_M), in fact, produces as an effect a proportional increase of the speed at the terminal of the damper and therefore, substantially, produces an increase of the forces produced by the same; the effect of the increase of the displacements produced by the leverage is, therefore, beyond a given value, compensated and exceeded by the increase of the forces inside the device connected because the increase of velocity, which tend to make the structure stiffer.

The α_k increase effect is clearly visible from Equation (15), from which it is evident that the structure undergoes an increase of the natural frequency and, therefore, of the stiffness.

From the examination of the graph of Figure 8, moreover, it can be deduced that the gain factor depends in a determining way on the dynamic characteristics of the structure and of the input force. The efficiency of the system is higher on stiffer structures, with an increasing efficiency as the natural frequency of the structure increases. The graph shows the mappings of the gain factor γ_d with the variation of the parameters α_k and α_d, for a $\alpha_M = 5$, for two different resonance frequencies of the structure, respectively 8 and 20, from which the described tendency is clearly visible. The gain factor γ_a presents similar behaviour. In any case, it should be noted that despite the system's improved efficiency, as the natural frequency of the system increases, the gain factors remain fairly stable (although increasing as ω increases) and this is a positive condition, which makes the system applicable to a wide range of structures. It should be noted, however, that as the natural frequency of the system increases, i.e., the stiffness of the structure, the cable system becomes increasingly expensive and difficult to implement, because of the need to increase the cable diameters and, therefore, the size of the diversion systems (pulleys) to maintain cable axial stiffness comparable to the bending stiffness of the bare structure.

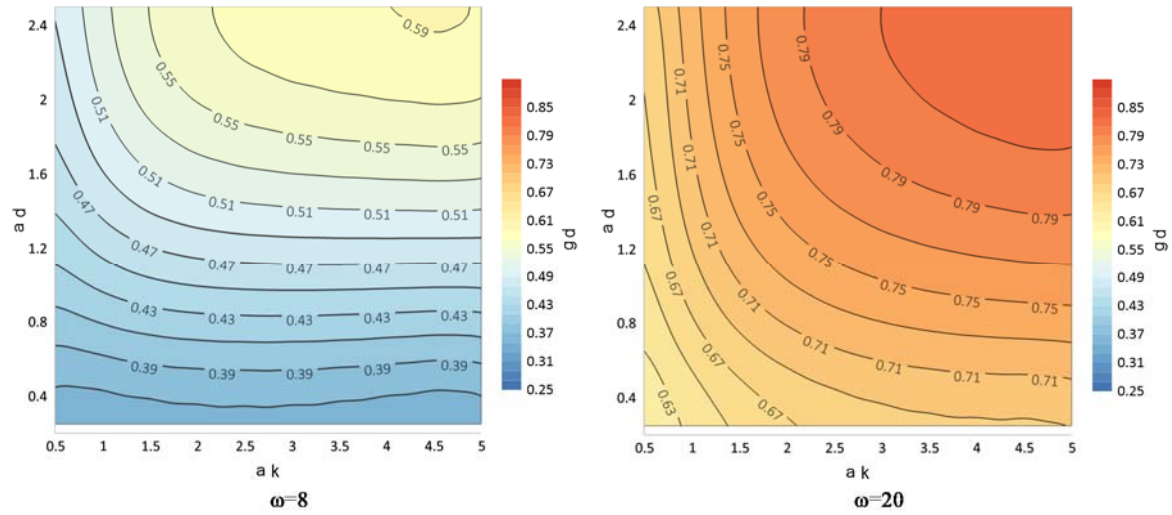

Figure 8. Gain maps in terms of γ_d for various ω values.

3.2. Numerical Examples

So far, only sinusoidal excitation with frequencies coinciding with the resonance frequency of the structure equipped with the damping system have been taken into account. In order to complete the theoretical analysis on the behavior of the system, the results of the time histories analysis conducted on the benchmark structure equipped with the damping system described in the previous paragraphs are illustrated below, with the following values of the coefficients $\alpha_d = 2$; $\alpha_k = 2$; $\alpha_M = 10$, with a input force consisting of a series of natural NTC (New Italian Technical Standards for constructions) spectum-compatible accelerograms [14], taken from a set of accelerograms extracted from the European Strong Motion Database (ESM), [15] through the REXEL software [16], for the L'Aquila site, adopting a type B soil category, in the range of periods between 0.15–2 s.

The first record is related to the seismic event named in ESM "Northwestern Balkan Peninsula" that occurred 15 April 1979 at 6:19:41 (UTC) in Montenegro with a thrust fault mechanism and a 6.9 Mw. The recording station was 16 kilometres from epicenter and recorded an event with duration of 23.91 s and peak ground acceleration of 3.68 m/s^2. The main frequencies content ranged from 1.5–6 Hz. The second was recorded from a station 7 km far from epicenter of the event that occurred 17 June 2000 in South Iceland, with 6.5 Mw and a strike slip fault mechanism. The record was 36.23 s long with a peak ground acceleration of 6.13 m/s^2. The main frequencies content ranged from 2–10 Hz.

From the examination of the results obtained, shown in Figure 9, with the application of natural forcing derived from the accelerograms recorded during the two seismic events indicated above, it emerges that the system allows consistent levels of dissipation to be reached, reducing the relative acceleration of the structure with respect to the base and the displacements of the same, in relation to the accelerations and displacements obtained for the bare structure. Of course, the extent of the reduction is closely related to the dynamic characteristics of the structure in relation to the dominant frequencies' content of the seismic input.

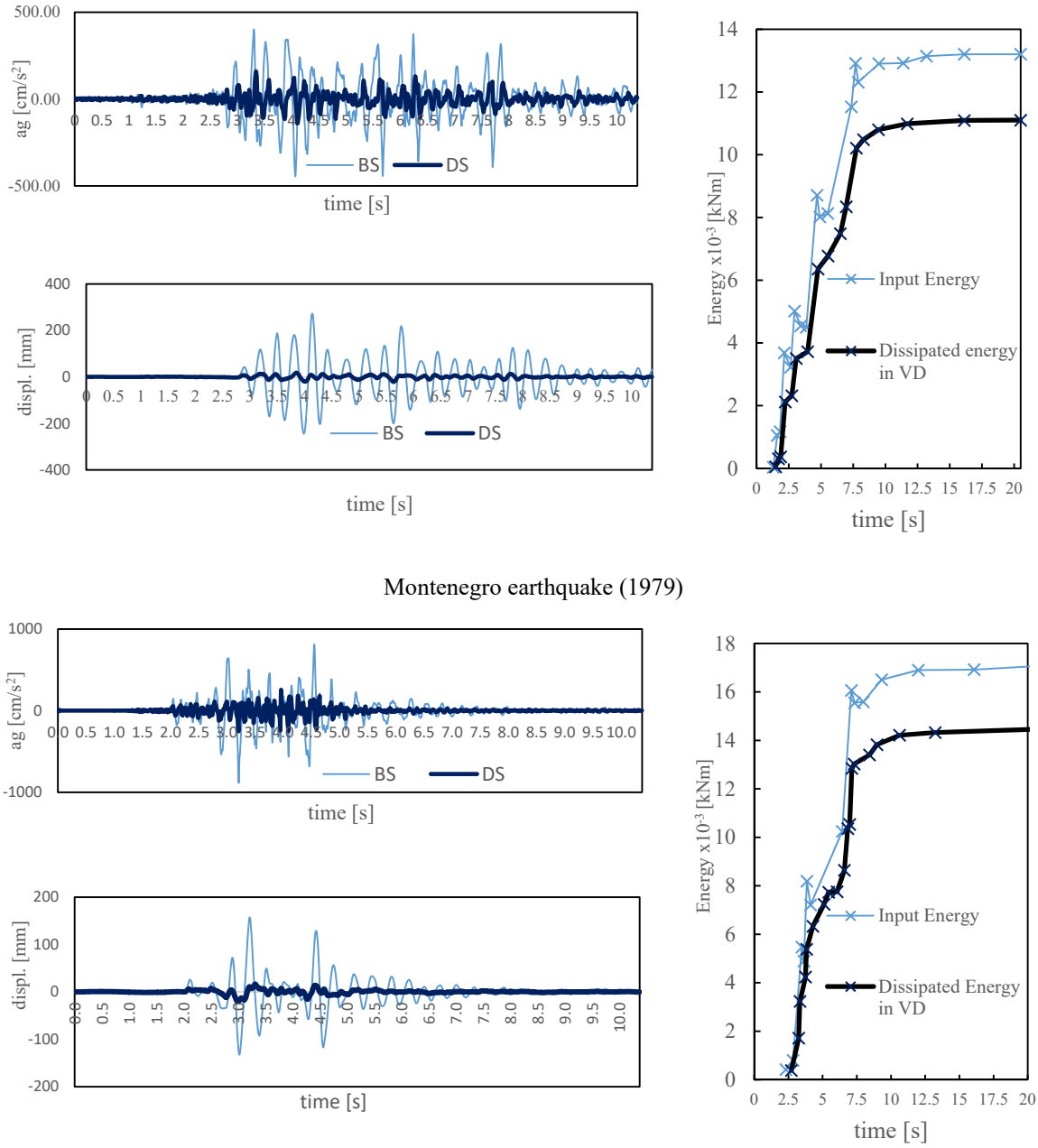

Figure 9. Roof displacement, acceleration and energy functions (input energy and dissipated energy in viscous damper device) obtained from time history analysis for bare SDOF structure (BS) and damped SDOF structure (DS), for various Italian NTC 2018 compatible spectra unscaled records.

4. Discussion

The results obtained both in the case of harmonic forces and in the case of natural excitation recorded in real seismic events confirm the good performance of the system in reducing the inter-story drifts and accelerations, fundamental features that determine stresses on the structural members, decrease or avoid damage also to the non-structural elements and improve comfort conditions inside the building during the seismic event. The main objective in the development of the described system is to be able to carry out a seismic retrofit of a building, implementing interventions exclusively from the outside, without proceeding to demolition of non-structural elements, finishes and systems. The system of cables, in fact, will be applied primarily on all the building prospects, anchored through clamps to the external nodes of the roof or, if necessary, to intermediate stories. In this way, the clamps

reaction is divided between the horizontal (beams) and vertical elements (columns) concurring into the node, stressing them with axial forces. The presence of rigid slabs in the structure also favors transferring seismic action to the frames equipped with the described system. Conversely, there is the possibility of interference between the path of the cables and architectural and functional projections present on the building prospect (balconies, etc.). Although variations to the cable path are possible, it is certainly easier to apply it on structures generally without such protrusions, but only windowed walls, such as schools or industrial buildings. In view of the importance that seismic vulnerability of existing school buildings assumes in many areas of the world and in particular in Italy, where most of the existing school heritage is characterized by seismic performance below the standards required by current regulations, we proceed in the following to the evaluation of the specific characteristics of some of the most common structural types in the school heritage in order to assess in advance and in simplified form the applicability and effectiveness of the proposed system.

The knowledge that authors have of the school building heritage of one of the Italian regions facing the greatest seismic hazard, Abruzzo, resulting from a collaboration with the regional civil protection officer, allows us to focus attention on some types considered most vulnerable, namely, buildings designed for gravity loads only in areas later identified with non-negligible seismic hazard. These buildings generally do not have the structural design and seismic details to allow a satisfactory performance during seismic events. These structures are generally made up of one-direction strong beams-weak columns frames, connected only by slabs in the transversal direction, with frequent pilotis floor, strip windows on the upper floors (Figure 10) and strong in plan and elevation structural irregularities. In the Abruzzo region, a large portion of coastal provinces of Teramo and Pescara were classified as "seismic areas" only in the last 20 years and therefore the majority of reinforced concrete school, built mainly in sixties and seventies, fall within this typology [17]. The situation described for Abruzzo can be extended to the whole country.

(**a**)Pilotis at ground floor and strip windows

(**b**)Very Strong beams–weak columns frame

(**c**)Squat column

(**d**)Mono-directional frame

Figure 10. General views of some existing school buildings in the Abruzzo region designed for gravity loads only.

In the following we take into account a early standard designed RC school building in Italy, which was also assumed as a benchmark structure for a research project financed by the Italian Department of Civil Protection [18,19], to check the applicability of the proposed system on it. The three-story structure was designed according to the 1980 edition of Italian Seismic Standards and completed in 1983. The interstory heights range from about 3.2 m to about 3.4 m, with intermediate story floors made of partly RC-prefabricated joists. The beams in the main frames, parallel to the longitudinal direction, have a section of (400 × 600) mm × mm; the column have a constant section of (500 × 400) mm × mm (Figure 11).

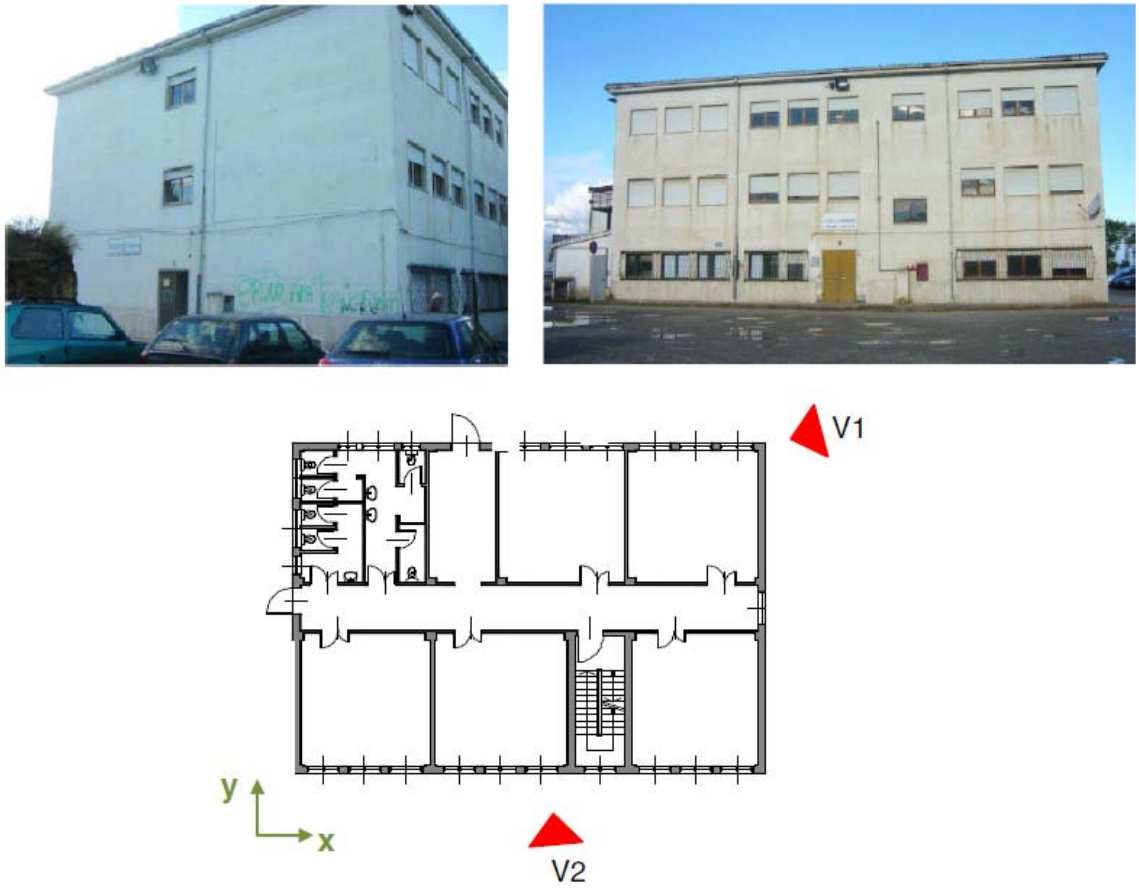

Figure 11. General views of the benchmark building and architectural plan of the floor type [19].

The objective of the system is to carry out a seismic retrofit mainly intervening from outside, without the need of non-structural elements, demolition or interruption to or limitation of the building's activity. Figure 12 shows a possible configuration of the cable system on the benchmark building main prospect. Each cable is connected to a different structure floor and transfers the displacement of each floor to the lever (pinned at the foundation beam), to which the viscous damper is connected. To do so, may be required a foundation enlargement also with micropiles in order to absorb the forces related to the diversion of the cable, when it does not occur at a beam-column joint, and do not increase shear forces in the foundation beam. As can be seen, despite the non-uniform spans of the frame beams, the system configuration can be effectively adapted without restricting accessibility in the building. The passage of cables at the windowed walls, although they produce a visual obstacle, does not reduce the functionality of the windows (opening from the inside) nor the light entry in the building. Other building prospects and, if needed, internal frames, will be equipped with similar cables layout.

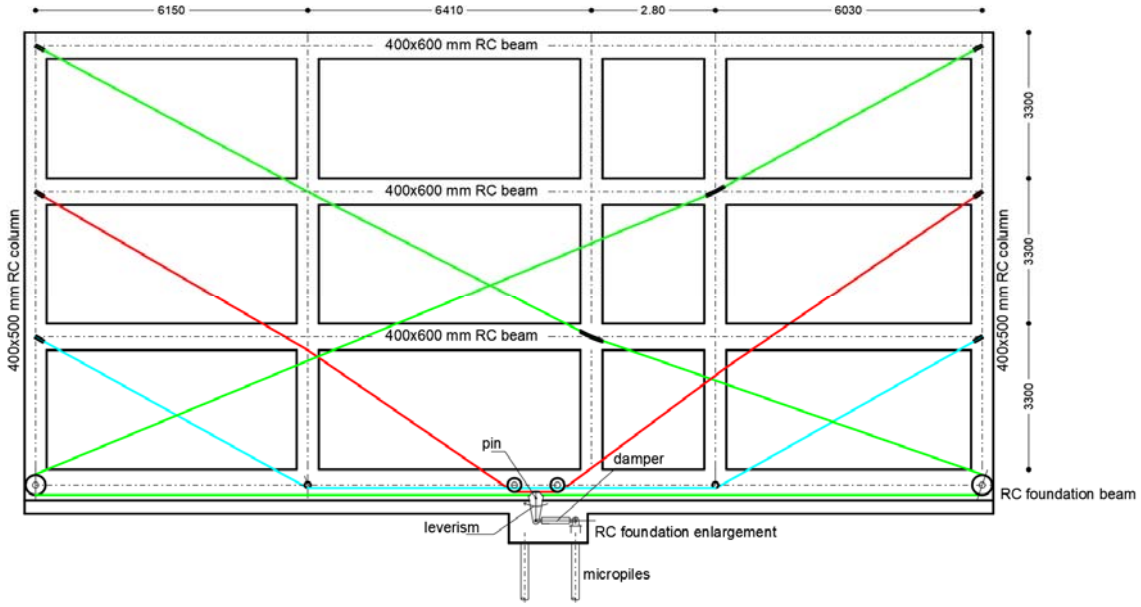

(**a**)

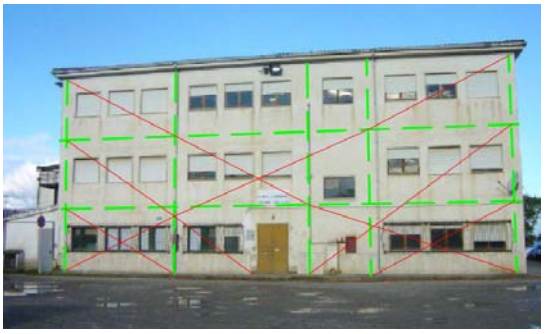

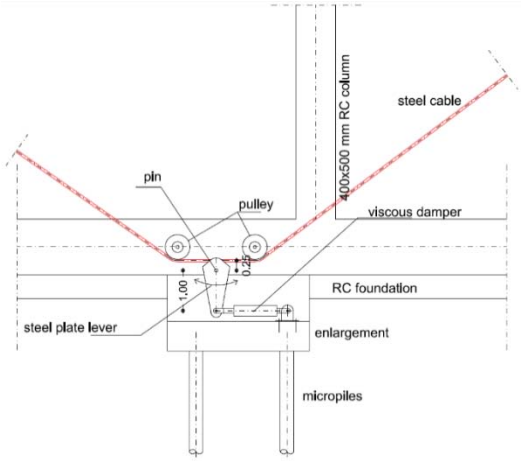

(**b**) (**c**)

Figure 12. (**a**) System layout on the main RC frame of the benchmark building: in green, red and cyan are represented, respectively, steel cables linking the 3th, 2th, and 1th floor to the foundation of the building; (**b**) Cable system layout depicted on the building prospect: steel cables (red lines), RC frame (dashed green lines); (**c**) transferring system of cable displacement to the viscous damper.

The system for transferring the cable displacements to the dissipation device is made by means of levers consisting of a specially shaped metal plate of suitable stiffness in order to limit its deformation, connected with the upper end to the cable and with the lower end to the viscous device. The length of the lever arms is such as to produce amplification of the displacements transferred by the cable to the device.

Further enhancement is expected from the use of non-linear viscous dampers, suitably calibrating their constitutive parameters [20] to reduce force peaks and increase dissipated energy.

Figure 13 shows the mean acceleration spectra obtained by a set of 7 NTC2018-spectrum compatible accelerograms extracted from the European Strong Motion Database, ESM [15] through the REXEL software in the case of a bare structure's SDOF-equivalent system with a 225,000 kg lumped mass (black line) and same structure equipped with the proposed system with the following values of the coefficients $\alpha_d = 2$; $\alpha_k = 2$; $\alpha_M = 10$ (red line). The figure shows the period range 0.3–0.6 s (blue

dotted line), which represent the variation range of the fundamental period of most existing reinforced concrete school buildings designed for gravity-loads only, in Teramo province (Abruzzo, Italy), and the proposed system significantly reduces inertial force on the structure.

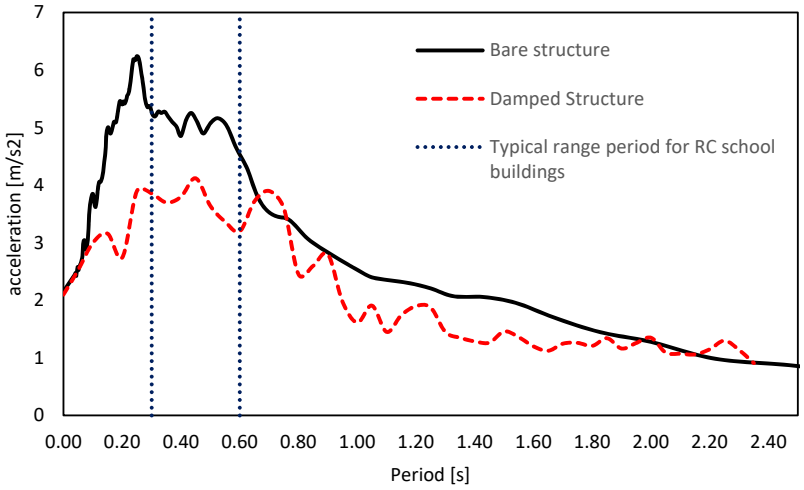

(**a**)

Waveform ID	Earthquake ID	Station ID	Earthquake Name	Mw	Fault Mechanism	Epicentral Distance [km]	PGA_X [m/s^2]	PGA_Y [m/s^2]	PGV_X [m/s]	PGV_Y [m/s]	EC8 Site class
232	108	ST77	Montenegro (aftershock)	6.2	thrust	20	0.56	0.5426	0.0363	0.0431	B
6263	1635	ST2484	South Iceland	6.5	strike slip	7	6.1359	5.018	0.3891	0.4975	B
1713	474	ST1257	Ano Liosia	6	normal	18	1.0872	0.839	0.1017	0.1045	B
131	63	ST28	Friuli (aftershock)	6	thrust	14	0.6498	1.2025	0.0543	0.0774	B
6328	2142	ST2484	South Iceland (aftershock)	6.4	strike slip	12	3.2645	3.8393	0.1988	0.2005	B
291	146	ST276	Campano Lucano	6.9	normal	16	1.5256	1.7247	0.271	0.2745	B
199	93	ST67	Montenegro	6.9	thrust	16	3.6801	3.5573	0.421	0.5202	B

(**b**)

Figure 13. (**a**) Mean acceleration spectra obtained by a 7 NTC-spectrum compatible accelerograms in the case of a bare structure's SDOF-equivalent system (black line) and same structure equipped with the proposed system with the following values of the coefficients $\alpha_d = 2$; $\alpha_k = 2$; $\alpha_M = 10$ (red dashed line); (**b**) Identification of the 7 NTC-spectrum compatible accelerograms.

Previous numerical analysis show that the presence of the amplification system is able to produce a significant increase in the displacements of the viscous device and allows the dissipation of a significant amount of energy, reducing the total displacements of the structure and the inter-story drift. The variations in the dynamic response of the structure, although present, are limited and in any case the natural frequency of the system does not undergo variations greater than 15%. This is particularly important, given the fact that mitigating structure stiffening makes it possible to avoid significant increases of inertia forces and the need for major reinforcement interventions on seismic resistant frame elements and foundations, condition, conversely, often required in case of dissipative braces arranged in the traditional way.

5. Conclusions

The present paper illustrates a seismic retrofit system for existing reinforced concrete structures by using additional viscous dampers connected to the structure by means of a system of cables and lever able to transmit the roof displacements to the base, where displacement amplification is carried out through a lever system and then transmitted to the dissipation device. The paper firstly deals with the simple case of a SDOF system in order to investigate the influence of the geometric characteristics of the structure and of the system, as well as of the characteristic parameters of the damper and of the stiffness ratios between the structure and the cables. The results show a high efficiency of the system already with axial stiffness of the cables of the order of 50% of the whole structure stiffness and for additional damping coefficients of the order of 20% of the internal structure damping coefficient. The amplification produced by the lever system appears to have a significant influence both on the dynamic characteristics of the structure equipped with the system, and on the amount of energy dissipated. The paper, furthermore, presents displacement and acceleration gain maps that can provide the first indications about the optimal system design. It is the aim of the authors to continue the research in order to investigate the effects on the system performances of the use of different dissipative devices (non-linear viscous and friction dampers, etc.) and their application to more complex structures and different typologies (prefabricated structures, masonry, bridges etc.) or different configurations of the cable system, and meanwhile carry on an experimental campaign to validate the results obtained in numerical analysis.

Author Contributions: A.S. and A.M. conceived the damping system after an idea of A.S.; A.M. defined the research methodology and validated results obtained from formal analysis carried out by A.S. and A.M.d.L. A.S. and A.M. wrote, edited and reviewed the paper. All authors have read and agreed to the published version of the manuscript.

Funding: This research received no external funding.

Conflicts of Interest: The authors declare no conflict of interest.

References

1. Constantinou, M.C.; Tsopelas, P.; Hammel, W.; Sigaher, A.N. Toggle-Brace-Damper Seismic Energy Dissipation System. *J. Struct. Eng.* **2001**, *127*, 105–112. [CrossRef]
2. Sigaher, A.N.; Constantinou, M.C. Scissor-Jack-Damper Energy Dissipation System. *Earthq. Spectra* **2003**, *19*, 133–158. [CrossRef]
3. Sorace, S.; Terenzi, G.; Frangipane, A. Incorporation of dissipative connections for seismic retrofit of reinforced concrete prefab structures. *Ing. Sismica* **2019**, *36*, 55–66.
4. Peckan, G.; Mander, J.B.; Chen, S.S. Balancing lateral loads using tendon-based supplemental damping system. *J. Struct. Eng.* **2000**, *126*, 896–905.
5. Peckan, G. Design of Seismic Energy Dissipation Systems for Reinforced Concrete and Steel Structures. Ph.D. Thesis, State University of New York, Buffalo, NY, USA, 1998.
6. Terenzi, G. Dynamics of SDOF systems with nonlinear viscous damping. *J. Eng. Mech.* **1999**, *125*, 956–963. [CrossRef]
7. Sorace, S.; Terenzi, G. Non-linear dynamic modelling and design procedure of FV spring-dampers for base isolation. *Eng. Struct.* **2001**, *23*, 1556–1567. [CrossRef]
8. Sorace, S.; Terenzi, G. The damped cable system for seismic protection of frame structures—Part II: Design and application. *Earthq. Eng. Struct. Dyn.* **2012**, *41*, 929–947. [CrossRef]
9. Naeem, A.; Kim, J. Seismic performance evaluation of spring viscous damper cable system. *Eng. Struct.* **2018**, *176*, 455–467. [CrossRef]
10. Saito, T.; Maegawa, T.; Denno, S.; Sakai, S.; Uchikawa, M.; Kanagawa, M.; Ryujin, H. New Seismic Response Control System Using Block and Tackle. In Proceedings of the 16th World Conference on Earthquake Engineering, 16WCEE, Santiago, Chile, 9–13 January 2017.
11. Berton, S.; Bolander, E.B. Amplification system for supplemental damping devices in seismic applications. *J. Struct. Eng.* **2005**, *131*, 979–983. [CrossRef]

12. Kang, J.; Tagawa, H. Seismic response of steel structures with seesaw systems using viscoelastic dampers. *Earthq. Eng. Struct. Dyn.* **2013**, *42*, 779–794. [CrossRef]
13. Newmark, N.M. A method of computation for structural dynamics. *J. Eng. Mech.* **1959**, *85*, 67–94.
14. Nuove Norme Tecniche Per le Costruzioni, New Italian Technical Standards for constructions. DM 17 January 2018. Available online: https://www.gazzettaufficiale.it/eli/gu/2018/02/20/42/so/8/sg/pdf (accessed on 20 January 2020).
15. Luzi, L.; Puglia, R.; Russo, E.; Orfeus WG5. *Engineering Strong Motion Database*; Version 1.0; Observatories & Research Facilities for European Seismology; Istituto Nazionale di Geofisica e Vulcanologia: Roma, Italy, 2016. [CrossRef]
16. Smerzini, C.; Galasso, C.; Iervolino, I.; Paolucci, R. Ground motion record selection based on broadband spectral compatibility. *Earthq. Spectra* **2013**, *30*, 1427–1448. [CrossRef]
17. Sabino, A.; Basi, M.; Marra, A.; Mannella, A. Analysis of the First Results of the Seismic Vulnerability Program of Schools in Abruzzo: State of Implementation and Issues Emerged. In Proceedings of the XVIII ANIDIS Conference, Ascoli Piceno, Italy, 15–19 September 2019.
18. Italian Department of Civil Protection. *Technical Report*; No. 031/10A.03; Italian Department of Civil Protection: Rome, Italy, 2005.
19. Sorace, S.; Terenzi, G. Motion control-based seismic retrofit solutions for a R/C school building designed with earlier Technical Standards. *Bull. Earthq. Eng.* **2014**, *12*, 2723–2744. [CrossRef]
20. Cavaleri, L.; Di Trapani, F.; Ferrotto, M.F. Experimental determination of viscous damper parameters in low velocity ranges. *Ing. Sismica* **2017**, *34*, 64–74.